Published in final edited form as:
Traffic. 2010 March ; 11(3): 348–360. doi:10.1111/j.1600-0854.2009.01022.x.

Gangliosides and β1-integrin are required for caveolae and membrane domains

Raman Deep Singh[1], **David L. Marks**[1], **Eileen L. Holicky**[1], **Christine L. Wheatley**[1], **Tatiana Kaptzan**[1], **Satoshi B. Sato**[2], **Toshihide Kobayashi**[3], **Kun Ling**[1], and **Richard E. Pagano**[1]

[1]Departments of Medicine; Biochemistry and Molecular Biology, Mayo Clinic College of Medicine, Rochester, MN 55905, USA

[2]Department of Biophysics, Kyoto University, Graduate School of Science, Kyoto 606-8502, Japan

[3]RIKEN, Wako, Saitama 351-0198, JAPAN

Abstract

Caveolae are plasma membrane domains involved in the uptake of certain pathogens and toxins. Internalization of some cell surface integrins occurs via caveolae suggesting caveolae may play a crucial role in modulating integrin-mediated adhesion and cell migration. Here we demonstrate a critical role for gangliosides (sialo-glycosphingolipids) in regulating caveolar endocytosis in human skin fibroblasts. Pretreatment of cells with endoglycoceramidase (cleaves glycosphingolipids) or sialidase (modifies cell surface gangliosides and glycoproteins) selectively inhibited caveolar endocytosis by >70%, inhibited the formation of plasma membrane domains enriched in sphingolipids and cholesterol ("lipid rafts"), reduced caveolae and caveolin-1 at the plasma membrane by ~80%, and blunted activation of β1-integrin, a protein required for caveolar endocytosis in these cells. These effects could be reversed by a brief incubation with gangliosides (but not with asialo-gangliosides or other sphingolipids) at 10°C, suggesting that sialo-lipids are critical in supporting caveolar endocytosis. Endoglycoceramidase treatment also caused a redistribution of focal adhesion kinase, paxillin, talin, and PIP Kinase Iγ away from focal adhesions. The effects of sialidase or endoglycoceramidase on membrane domains and the distribution of caveolin-1 could be recapitulated by β1-integrin knockdown. These results suggest that both gangliosides and β1-integrin are required for maintenance of caveolae and plasma membrane domains.

Keywords

caveolar endocytosis; glycosphingolipids; caveolin-1; sialidase; endoglycoceramidase; focal adhesions

Introduction

Many endocytic entry pathways into cells have been identified. These vary in the cargo molecules they transport and the underlying protein machinery that facilitates the different endocytic processes (1–3). Among the clathrin-independent mechanisms of endocytosis, caveolar uptake is perhaps the best studied. Caveolae are 50–80 nm diameter flask-shaped plasma membrane (PM)[1] invaginations that are marked by the presence of a member of the caveolin (Cav) protein family (4) and by PTRF-Cavin, a putative caveolar coat protein that is

Corresponding author: Dr. Richard E. Pagano, Mayo Clinic College of Medicine, 200 First Street, S.W., Rochester, MN 55905-0001. Tel: (507) 284-8754; Fax: (507) 266-4413; pagano.richard@mayo.edu.

thought to be required for caveola formation (5,6). Markers used to visualize uptake through caveolae include labeled albumin (7–9), SV40 virus (10), and in some cell types, the cholera toxin B (CtxB) subunit (8,11,12). In addition, we and others have provided evidence that a fluorescent analog of lactosylceramide [*N*-(4,4-difluoro-5,7-dimethyl-4-bora-3a,4a-diaza-s-indacene-3-pentanoyl)sphingosyl 1-β-D-lactoside; Bodipy-LacCer], and other glycosphingolipid (GSL) analogs, are internalized almost exclusively *via* caveolae in human skin fibroblasts (HSFs) and other cell types based on multiple approaches (8,9,13–15).

Although the importance of caveolar endocytosis is now well appreciated, the regulation of this process is not fully understood. Several factors however are known to play an important role in this process. First, caveolar endocytosis is stimulated when cells are treated with phosphatase inhibitors (e.g., okadaic acid) or when certain caveolar cargo binds to its receptor (16,17). Stimulation of caveolar endocytosis is accompanied by increased activation of src and phosphorylation of caveolin-1 (Cav1) and dynamin (18), suggesting that stimulation occurs *via* increased kinase activities. In agreement with this notion, a screen of the human kinome identified a total of 80 different kinases that are somehow involved in the uptake of SV40 virus, a caveolar marker (19). Second, stimulation of caveolar endocytosis occurs when cells are briefly incubated with either natural or synthetic GSLs such as bovine GM_1 ganglioside, bovine LacCer, D-Lactosyl-β1-1'-N-octanoyl-D-*erythro*-sphingosine (C8-D-*erythro*-LacCer), or Bodipy-LacCer (9,20). A third important factor for caveolar endocytosis is that this process is regulated by microdomain clustering. This notion is supported by the findings that (i) treatments that promote clustering of cargo (e.g., SV40 virus, cholera toxin B subunit (CtxB) crosslinking, D-*erythro*-LacCer) in microdomains can also stimulate caveolar endocytosis (4,9,21,22). In contrast, treatments that inhibit clustering in microdomains (e.g., methyl-β-cyclodextrin, filipin, C8-L-*threo*-LacCer) inhibit endocytosis via caveolae (9,11,21,23).

In the current study we examine the role of endogenous cell surface gangliosides and show that they also play a key role in regulation of caveolar uptake. Gangliosides are sialylated glycosphingolipids (GSLs); they are highly diverse because of the various combinations of carbohydrate building blocks, linkage position, number and position of sialic acid residues, and the precise molecular structure of the ceramide lipid anchor (24). In addition to serving as receptors for certain viruses and toxins, gangliosides have also been shown to participate in a number of complex cellular processes including cell-cell interactions and regulation of certain growth factor receptors (e.g., epidermal growth factor and the insulin receptor) (25). Importantly gangliosides are not only components of PM domains including caveolae, but they can interact with integrins (26,27) sometimes in association with other transmembrane proteins (e.g., the tetraspanins), and they can modulate integrin-based cell attachment (28). Here we demonstrate for the first time that gangliosides are required for the maintenance of PM caveolae and for caveolar endocytosis, and show that they regulate the organization of PM microdomains, β1-integrin activation, and focal adhesion assembly.

Results

Cell surface sialic acid residues support caveolar endocytosis

To study the effects of loss of cell surface sialic acids on endocytic pathways, human skin fibroblasts (HSFs) were treated with sialidase from *Arthrobacter ureafaciens* which cleaves

[1]**ABBREVIATIONS**: **Bodipy-LacCer**, *N*-(4,4-difluoro-5,7-dimethyl-4-bora-3a,4a-diaza-s-indacene-3 pentanoyl)sphingosyl 1-β-D-lactoside; **C8-ceramide**, *N*-octanoyl-D-*erythro*-sphingosine; **C8-D-*erythro*-LacCer**, β-D-lactosyl-*N*-octanoyl-D-*erythro*-sphingosine; **C8-L-*threo*-LacCer**, β-D-lactosyl-*N*-octanoyl-L-*threo*-sphingosine; **Cav1**, caveolin-1; **CHO**, chinese hamster ovary; **CtxB**, cholera toxin, B subunit; **EGCase**, endoglycoceramidase; **FAK**, focal adhesion kinase; **GSL**, glycosphingolipid; **HSFs**, human skin fibroblasts; **IL-2R**, interleukin-2 receptor β subunit; **LacCer**, lactosylceramide; **L-*threo*-LacCer**, β-D-lactosyl-*N*-octanoyl-L-*threo*-sphingosine; **PIPKI**γ, Type Iγ phosphatidylinositol phosphate kinase; **PM**, plasma membrane; **PTRF**, polymerase I and Transcript Release Factor; **Tfn**, transferrin.

the terminal N-acetylneuraminic acid residues from the cell surface glycoproteins and gangliosides [(29); Supp. Fig. S1]. After sialidase treatment, cells were incubated with various markers for uptake *via* clathrin-dependent or clathrin-independent endocytosis (1). Pretreatment with sialidase dramatically inhibited internalization of Bodipy-LacCer (Fig. 1A;Supp. Fig. S2A), a marker for caveolar endocytosis (8,9,13–15,30). Lipid extraction and analysis demonstrated that approximately equal amounts of Bodipy-LacCer became cell-associated at 10°C in untreated (control) vs sialidase-treated cells, demonstrating that the inhibition of caveolar endocytosis by sialidase was not due to lower levels of PM labeling with Bodipy-LacCer prior to endocytosis at 37°C (Supp. Fig. S2B). In addition, sialidase pretreatment had no effect on internalization of markers for the clathrin pathway (Tfn; Fig. 1A), for fluid phase uptake (dextran and GFP-GPI), or RhoA-dependent uptake of the IL-2Rβ (Fig. 1B). In contrast, pretreatment with trypsin had no effect on Bodipy-LacCer or dextran internalization but significantly inhibited endocytosis of Tfn, GFP-GPI and IL-2Rβ, presumably due to direct proteolytic cleavage of the cell surface proteins (e.g., Tfn receptor, GFP-GPI) being monitored (Fig. 1A,B).

To further test the role of cell surface sialic acid residues on endocytosis, we also examined endocytosis in Lec2 cells, a mutant Chinese hamster ovary (CHO) cell line unable to translocate CMP-sialic acid to the lumen of the Golgi apparatus and consequently deficient in sialic acid-containing glycoproteins and glycolipids vs the parental CHO Pro5 cell line (31). As shown in Fig. 1C,D, there was a drastic reduction in Bodipy-LacCer endocytosis in Lec2 cells vs Pro5 cells, whereas Tfn uptake was unaffected and dextran internalization was somewhat elevated relative to that in the CHO (Pro5) control cells. The strong inhibition of caveolar endocytosis in Lec2 cells is consistent with the results of sialidase treatment of HSFs shown in Fig. 1A,B.

Since sialidase pretreatment and the Lec2 mutation affect both cell surface GSLs and glycoproteins, we next examined the effect of endoglycoceramidase (EGCase) on endocytosis as this enzyme only modifies GSLs (i.e., hydrolyzes the linkage between the oligosaccharide and ceramide of acidic and neutral GSLs; see Fig. S1) but not proteins. Similar to the results using sialidase, pretreatment of cells with EGCase selectively inhibited caveolar endocytosis of Bodipy-LacCer but had no effect on internalization by other mechanisms (Fig. 1A,B), suggesting that cell surface sialic acid-containing lipids (i.e., gangliosides) rather than proteins might be responsible for the observed effects on caveolar endocytosis. This inhibition was not due the formation of ceramide by EGCase, since incubation of untreated cells with C8-ceramide did not significantly inhibit uptake of Bodipy-LacCer (Supp. Fig. S2C,D). To examine the effect of sialidase and EGCase treatments on endocytosis of Bodipy-LacCer further, we attempted to reverse their effects by incubating the enzymatically-treated cells with a panel of GSLs prior to monitoring LacCer endocytosis. Addition of individual gangliosides (i.e., sialic-acid containing GSLs such as GM_1, GM_2, GD_{1a}) as well as ganglioside mixtures restored Bodipy-LacCer endocytosis in sialidase- and EGCase-treated cells, whereas neutral GSLs (e.g., asialo-GM_1, asialo-GM_2, C_8-D-*e*rythro-LacCer) or neutral GSL mixtures were not able to restore Bodipy-LacCer uptake (Fig. 2). Importantly, no restoration of caveolar endocytosis was seen when sulfatide (a negatively-charged SL; see Fig. S1) was used (Fig. 2B), suggesting that restoration did not simply result from the presence of negatively charged lipids at the PM. Together the results in Fig. 1 and Fig 2 demonstrate that sialidase and EGCase exert their effects on endocytosis by altering cell surface gangliosides, and that these lipids are critical in supporting caveolar endocytosis.

Effect of sialidase and EGCase treatments on caveolae and Cav1

We examined the effect of sialidase and EGCase treatments on PM caveolae by transmission electron microscopy. For these studies, samples were prepared using Ruthenium Red to identify caveolae connected to the cell surface as described (32). The number of caveolae, defined as

uncoated surface invaginations between 50 and 80 nm in diameter, was counted in a blinded manner. As shown in Fig. 3, control HSFs showed numerous caveolae on both the dorsal (heavily stained) and ventral (lightly stained) surfaces of the PM whereas treatment with sialidase or EGCase for 30 min at 37°C (identical conditions to those used in Fig. 1 and Fig 2) reduced the number of PM caveolae by ~80 %.

We next used immunofluorescence to examine the effects of sialidase and EGCase pretreatments on the intracellular distribution of Cav1 using an antibody and fixation-permeabilization protocol to stain endogenous Cav1 pools at both the Golgi apparatus and cell surface (33). When control cells were examined by TIRF microscopy strong staining at the PM was seen, while in sialidase-and EGCase-treated cells, Cav1 staining of the cell surface was significantly reduced (Fig. 4A). A similar result was obtained using another antibody and staining protocol specific for the PM pool of Cav1 (33) (data not shown). Furthermore, real time (TIRF) imaging of HSFs expressing Cav1-GFP showed a rapid decrease in Cav1 at the PM during the first few minutes of sialidase treatment at 37°C, whereas in untreated control cells, no changes were observed over the same time period (Fig. 4B). Western blotting of cells further demonstrated that the total endogenous Cav1 pool was not diminished by the enzyme treatments (Fig. 4C), and epifluorescence images of the cells demonstrated that Cav1 had redistributed into cytoplasmic pools. Furthermore, incubation of EGCase-treated cells with exogenous GM_1 ganglioside for 30 min at 10°C (identical conditions to those in Fig. 2 that restored caveolar endocytosis) induced endogenous Cav1 to redistribute back to the PM (Fig. 4D,E).

In agreement with published studies, we also found that PTRF-Cavin (5,6), a caveolar protein, co-localized with Cav1 at the PM in control cells (Fig. 5). However, in sialidase and EGCase treated cells, Cav1 was redistributed to the Golgi apparatus while PTRF-Cavin showed a non-overlapping diffuse and punctate distribution in the cells (Fig. 5). Taken together, the results in Fig. 3–Fig 5 demonstrate that sialidase and EGCase treatments reduced PM caveolae and caused a redistribution of key proteins normally associated with caveolae, providing a structural basis for the observed inhibition of caveolar endocytosis. Importantly, exogenous sialic acid-containing gangliosides restored the distribution of Cav1 at the PM in the enzyme-treated cells (Fig. 4D,E) providing a basis for restoration of caveolar endocytosis in these cells.

Disruption of PM domains by sialidase and EGCase treatment

We have shown that clustering of lipids and proteins into GSL- and cholesterol-enriched micron-size domains (or “rafts”) at the PM can be monitored using Bodipy-LacCer [reviewed in (34)], and that such domains are required for caveolar endocytosis in HSFs (21). Thus, we next sought to learn whether these PM microdomains were altered by sialidase and EGCase treatments. To do so, after sialidase or EGCase pretreatments, cells were incubated with Bodipy-LacCer for 30 min at 10°C, and live cell images were acquired at 10°C to inhibit endocytosis. To distinguish PM domains enriched in LacCer from other regions of the PM containing lower concentrations of the lipid analog, we simultaneously monitored both monomer (green; low concentration) and excimer (red; high concentration) fluorescence [Fig. 6 and (34,35)]. In control cells, Bodipy-LacCer was enriched in numerous micron size “clusters” which exhibited yellow/orange fluorescence, while neighboring regions of the cell surface that contained less of the lipid analog fluoresced green. In contrast, pretreatment of cells with EGCase or sialidase resulted in loss of the yellow/orange clusters of fluorescence at the PM indicating a reduction or loss of micron-size PM clusters (Fig. 6;Supp. Fig. S3A). As noted above, lipid extraction and analysis further demonstrated that the amount of fluorescent LacCer that became cell-associated at 10°C was not affected by pretreatment of HSFs with sialidase or EGCase (Supp. Fig. S2B). Importantly, when the enzymatically-treated cells were subsequently incubated with GM_1 ganglioside at 10°C followed by incubation with Bodipy-

LacCer, the micron-size clusters of yellow/orange fluorescence at the PM were again visible (Fig. 6). However, this restoration of PM domains was not observed when cells were incubated with asialo-GM_1 ganglioside (Fig. 6A,B). These experiments demonstrate that the presence of sialic acid residues on lipids is required for PM domains as monitored by clustering of Bodipy-LacCer. We also used PEG-cholesterol as another marker for PM domains (36) and found that this probe was (i) enriched in micron-size clusters at the PM of control cells similar in appearance to those seen using Bodipy-LacCer, and (ii) these clusters were lost when cells were pretreated with EGCase (Supp. Fig. S3B,C).

Effect of EGCase and Sialidase treatments on integrin activation and focal adhesions

In a previous study we showed that a non-natural stereoisomer of LacCer inhibits caveolar endocytosis, blocks the clustering of lipids and proteins into GSL- and cholesterol-enriched PM domains, and blunts β1-integrin activation (21). Since these first two effects were seen in HSFs treated with sialidase or EGCase (Fig. 1 and Fig 6), we next examined the effects of EGCase treatment on β1-integrin activation and on the distribution of several components of the focal adhesion complex (Fig. 7 and Fig 8). To examine integrin activation we used HUTS-4, a monoclonal antibody that binds to β1-integrins in their activated conformation. Untreated cells grown in serum-containing medium showed a basal level of integrin activation that was significantly reduced in EGCase-treated cells (Fig. 7A,B). However EGCase treatment did not alter the PM levels of β1-integrin detected by immunofluorescence (Fig. 7C,D) or the total levels of β1-integrin detected by Western blotting (Fig. 7E). Importantly, this inhibition of integrin activation was partially restored when EGCase treated cells were incubated with exogenous GM_1 ganglioside (Fig. 7A,B). Treatment with EGCase caused a redistribution of focal adhesion kinase (FAK), pFAK, Type Iγ phosphatidylinositol phosphate kinase (PIPKIγ), paxillin, and talin away from focal adhesions (Fig. 8A,B), while no change in the total cellular levels of each of these proteins was seen by Western blotting (Fig. 8C). Together the data in Fig. 7 and Fig 8 demonstrate that EGCase treatment inhibited β1-integrin activation, and disrupted the localization of several key proteins found in focal adhesion complexes.

Knockdown of β1-integrin

In a previous study using HSFs, we showed that depletion of β1-integrin inhibited clustering and activation of this integrin and blocked caveolar endocytosis (21). Since pretreatment of HSFs with EGCase also blunts activation of β1-integrin and inhibits caveolar endocytosis, we next examined the effect of β1-integrin knockdown on PM domains and on the distribution of Cav1. Using an siRNA approach (21), we depleted β1-integrin > 95% (Supp. Fig. S4). No effects of β1-integrin knockdown on cell attachment were observed, presumably because of the presence of other integrins and other adhesion proteins in the HSFs. We then incubated these cells with Bodipy-LacCer or AF647 PEG-Chol to observe the effect of the knockdown on PM domains. Micron-size clusters of Bodipy-LacCer or PEG-Chol were readily apparent in untreated control cells and in cells transfected with a negative siRNA, but were almost completely eliminated in β1-integrin-depleted cells using either domain marker (Fig. 9A–C). β1-integrin depletion also caused a redistribution of Cav1 from the PM to intracellular membranes (Fig. 9D,E). The loss of micron-size PM domains and redistribution of Cav1 away from the PM in β1-integrin-depleted cells (Fig. 9) were similar to the effects seen when HSFs were treated with EGCase (Fig. 4, Fig 6). These results suggest that β1-integrins are required for the formation of PM domains and Cav1 association with the PM. However, incubation with exogenous GM_1 ganglioside at 10°C did not induce the redistribution of Cav1 back to the PM (Fig. 9D,E), suggesting that both gangliosides and β1-integrin are required for this process to occur.

Discussion

In the present study we found that enzymatic depletion of cell surface sialic acid residues using sialidase or EGCase inhibited caveolar endocytosis in HSFs, but did not affect other mechanisms of internalization. Caveolar endocytosis was also inhibited in a mutant CHO cell line deficient in the synthesis of sialic acid-containing glycoproteins and glycolipids, suggesting that the effects reported here are not limited to HSFs. We were able to attribute this inhibition to depletion of gangliosides, rather than a loss of sialic acid residues from glycoproteins for several reasons. First, when cells were incubated with EGCase which modifies cell surface GSLs but not proteins (37,38), virtually identical results were obtained to those found using sialidase [e.g., on endocytosis (Fig. 1), or on the loss of PM caveolae and Cav1 (Fig. 3–Fig 4)]. Second, the effects of sialidase treatments on endocytosis could be reversed by exogenous GM_1 and other gangliosides, but not by asialo-gangliosides or neutral GSLs (Fig. 2). It is important to note that cell surface gangliosides have been shown to act as receptors for the uptake of certain pathogens [e.g., SV40 virus and Cholera toxin and *Mycoplasma pneumoniae*; (4,39–41)]. Subsequent entry of many of these pathogens usually occurs by a clathrin-independent mechanism such as caveolar endocytosis (40,42,43) and perturbation of the PM domains (e.g., by cholesterol depletion) can inhibit internalization of the pathogen (44). However, to our knowledge, our study is the first to show that PM gangliosides are required for caveolar endocytosis as well as the maintenance of PM Cav1 and caveolae (Fig. 1,Fig 3,Fig 4).

Treatment of HSFs with sialidase or EGCase inhibited caveolar endocytosis (Fig. 1), but also had other effects that may be related to blocking this endocytic mechanism. These include (i) inhibition of PM domains, (ii) loss of Cav1 from the PM, and (iii) inhibition of β1-integrin activation (Fig. 4, Fig 6, Fig 7). Each of these effects could be reversed by incubation with an exogenous ganglioside. A major open question regarding the underlying mechanism for ganglioside regulation of caveolar endocytosis is whether gangliosides affect each of these processes independently, or whether there is a temporal sequence of events in which ganglioside depletion inhibits one process and disruption of that process in turn blocks other processes leading to the eventual inhibition of caveolar endocytosis. For example, the primary effect of ganglioside depletion could be to block PM domain formation with the absence of PM domains preventing activation of β1-integrin and the formation of caveolae. Another possibility is that the loss of gangliosides transiently stimulates the endocytosis of caveolae and related microdomains at the PM, similar to the effects of cell detachment on internalization of caveolae reported by del Pozo et al. (45) These issues may be further explored in future studies by treating cells with sialidase or EGCase at various (low) concentrations or for various times to achieve different levels of ganglioside depletion. For a given level of depletion, temporal changes in PM domains, activation of β1-integrin, and loss of endogenous Cav1 from the PM could then be examined. Results from these studies may indicate whether these processes are sequential (e.g., does loss of PM domains precede loss of Cav1 from the PM) and possibly linked, or whether all of these events occur simultaneously suggesting they may be independent of one another.

In summary, this study demonstrates that PM gangliosides can selectively regulate caveolar endocytosis and related processes in HSFs. The regulation of caveolae and microdomains by gangliosides could be physiologically important as there are many reports of changes in gangliosides in normal or pathological states. For example, endogenous sialidases (e.g., Neu3) which play key roles in cancer and differentiation (46) could function by regulating microdomain based signaling. In addition, certain tumor cells express aberrant levels and species of gangliosides (47,48) and shed these gangliosides into the tumor microenvironment thus affecting surrounding cells (49,50). Such changes in gangliosides could affect tumor

invasiveness, focal adhesion formation and angiogenesis by modulating the formation of caveolae or integrin signaling.

Materials and Methods

Cell Culture

Normal HSFs (GM-5659; Coriell Institute for Medical research, Camden, NJ) were grown as described (21). CHO mutant (Lec-2) and parental (Pro-5) cell lines were purchased from ATCC (Manassas, VA), and maintained per instructions supplied by the ATCC. All experiments were performed using monolayer cultures grown to ~40–60% confluency on acid-etched glass coverslips.

Lipids, Fluorescent Probes and Miscellaneous Reagents

Bodipy-D-*e*-LacCer was synthesized, purified and subsequently complexed to defatted bovine serum albumin (DF-BSA) for incubation with cells (30). Fluorescent Alexa Fluor (AF) 594 labeled-transferrin (Tfn), AF594-dextran (10kD), Ab labeling kits, and fluorescent secondary Abs were from Invitrogen (Eugene, OR). Anti GFP (IgG1) antibodies were from Sigma (San Diego, CA). Anti GFP Fab fragments were generated from this IgG_1 using the Immunopure IgG_1 Fab preparation kit from Pierce Biotechnology (Rockford, IL) and were labeled with AF647 succinimidyl ester using a protein labeling kit from Invitrogen. PIPLCγ (Phosphatidylinositol phospholipase Cγ) was purchased from Sigma Chemical Co. Antibodies were purchased from BD Biosciences (San Jose, CA; β1-integrin, Paxillin, FAK, and pFAK), Millipore (Billerica, MA; HUTS-4 β1-integrin), and Sigma Chemical Co. (St. Louis, MO; Talin). Anti PIPK1γ was obtained as described (51). Sialidase was from Sigma Chemical Co. and Glyko Biochemicals; EGCase was from Takara Biochemicals and Sigma Chemical Co. All other reagents were from Sigma-Aldrich.

Constructs and transfection experiments

DNA constructs encoding GPI-GFP and IL-2R were gifts from J. Lippincott-Schwartz (NIH, Bethesda, MD) and A. Dautry-Varsat (Institute Pasteur, Paris, France), respectively. HA-tagged PIPKIγ was described previously (51). Transfection of DNA constructs was performed using a Nucleofector II apparatus (Amaxa Biosystems).

β1-integrin knockdown

siRNAs for β1-integrin (ON-TARGETplus SMARTpool L-004506-00) and negative siRNA (ON-TARGETplus Non-targeting siRNA D-001810-01-05)) were purchased from Thermo Scientific. Knockdown in HSFs was performed using 360 pmol/ml siRNA with DharmaFECT 2 transfection reagent (Thermo Scientific) as per supplier's instructions. Knockdown was confirmed by Western blotting and immunofluorescence 72 h after transfection as shown in Supp. Fig. S4. All further experiments were also performed 72 h after transfection.

Enzymatic treatments of intact cells

HSFs were pretreated with sialidase (0.1 unit/ml medium) or EGCase (20 milliunits/ml medium) for 30 min at 37°C at pH 5.5, washed, and returned to pH 7.2 medium. Control cells were treated identically at the same pH without enzyme. Cells were then washed and pH adjusted to 7.2 for further binding and endocytosis assays. In some experiments, cells were pretreated with 0.01% trypsin (Trypsin type II tablets; Sigma Chem. Co) for 30 min at 37°C, followed by 5% BSA for inactivation of the enzyme. Cells were then washed and further used for various endocytosis or signaling assays as described elsewhere in Materials and Methods. No apparent effect on cell viability was seen for any of these treatments.

Endocytosis assays

For endocytosis of Bodipy-LacCer or Alexa fluor (AF) labeled Tfn, HSFs upon pretreatments (with either enzymes or with trypsin) were incubated with the fluorescent marker for 30 min at 10°C, washed and further incubated for 3 min at 37°C (21). For AF labeled dextran, cells were incubated for 5 min at 37°C without pre-incubation after the pretreatment. Endocytosis of IL-2R was performed as described previously (14). For GPI-anchored protein uptake, HSFs were first transfected with GPI-GFP for 48 hrs and then were pretreated as above. Cells were then incubated with AF647-labeled anti-GFP-Fab for 30 min at 10°C, washed and incubated for 5 min at 37°C. Cells were then treated with PIPLCγ (Phosphatidylinositol phospholipase Cγ) (Sigma Chemical Co) to remove cell surface GPI-GFP. All other samples were either acid stripped or back exchanged to remove cell surface fluorescence before fluorescence microscopy. Endocytosis of Bodipy-LacCer, AF labeled Tfn and dextran was carried out identically in mutant Lec-2 and their parental cell line Pro-5.

Electron Microscopy

For EM studies, HSFs were grown on Aclar sheets placed in 35-mm culture dishes and were either untreated (control) or treated with sialidase or EGCase for 30 min at 37°C (see above). Samples were then fixed in the presence of 1 mM ruthenium red and embedded as described (20). Transverse ultrathin sections were cut and viewed under a FEI Tecnai T12 transmission electron microscope operating at 80 kV. Overlapping images of the entire cell perimeter in a given field were taken at 15,000 × magnifications. For quantitation, the number of ruthenium red positive, 50 to 80 nm-diameter vesicles within 0.5 μm of the cell surface were counted for the entire cell perimeter. Values are expressed per 100 μm of perimeter length.

Microdomain Studies

HSFs were washed with ice cold HMEM and were pretreated with or without sialidase or EGCase for 30 min at 37°C. Cells were then washed and incubated with 2.5μM Bodipy-LacCer for 30 min at 10°C to label the PM. Samples were then washed, and images were acquired simultaneously at green and red wavelengths using a Dual-View module (Optical Insights; Tucson, AZ). For glycolipid supplementation, cells were incubated with GM_1 (as described below) for 30 min at 10°C after enzyme pretreatment. Cells were then washed and further incubated with 2.5 μM Bodipy-LacCer for 30 min at 10°C, washed and imaged as above.

Glycolipid supplementation assay

Different lipids (20 μg/ml), as indicated, were dissolved in EtOH:DMSO ⁜ 1:1 and were added in HMEM+G and incubated after different pretreatments as indicated for 30 min at 10°C. Cells were then washed three times and processed for further endocytosis, microdomains or restoration of Cav1 at the PM.

Fluorescence Microscopy and Analysis

Fluorescence microscopy was performed using a fluorescence microscope (I×70; Olympus) equipped with 60× 1.4NA or 100× 1.35 NA oil immersion objectives. Images were acquired using a Quant EM: 512SC (Photometrics) CCD camera. For quantitation, all photomicrographs in a given experiment were exposed and processed identically for a given fluorophore and were analyzed using the MetaMorph image processing program (version 7.3.2; Universal imaging Corp.). Quantitative results are expressed as mean ± SDs. Images were prepared for individual figures using Photoshop CS (Adobe). Total internal reflection fluorescence (TIRF) microscopy was carried out using an Olympus attachment for the I×70 microscope. No deconvolution, 3D reconstructions, surface or volume rendering, or gamma adjustments were performed. Some micrographs in Fig. 8 were obtained using a Zeiss LSM510 confocal microscope equipped

with 100× 1.3NA lens. Details regarding fluorophores and temperature are given in the text or figure legends.

Miscellaneous procedures

SDS-PAGE and immunoblotting of cell lysates and immunofluorescence of formaldehyde- or methanol-fixed cells were performed as described previously (21,33). Lipid extraction and thin layer chromatography analysis (TLC) were performed as described (52). SLs were separated by TLC and identified by comparison to known standards using $CHCl_3/CH_3OH$/15 mM $CaCl_2$ (65:35:8; v/v/v) as the developing solvent. Primulin or resorcinol was used as a detection reagent, and lipids were quantified by scanning densitometry (53).

Supplementary Material

Refer to Web version on PubMed Central for supplementary material.

Acknowledgments

This work was supported by the Mayo Foundation and grants from the NIH Grants GM-22942 and GM-60934 to REP.

References

1. Mayor S, Pagano RE. Pathways of clathrin-independent endocytosis. Nat Rev Mol Cell Biol 2007;8:603–612. [PubMed: 17609668]
2. Doherty GJ, McMahon HT. Mechanisms of endocytosis. Annu Rev Biochem 2009;78:857–902. [PubMed: 19317650]
3. Hansen CG, Nichols BJ. Molecular mechanisms of clathrin-independent endocytosis. J Cell Sci 2009;122(Pt 11):1713–1721. [PubMed: 19461071]
4. Pelkmans L, Helenius A. Endocytosis via caveolae. Traffic 2002;3:311–320. [PubMed: 11967125]
5. Hill MM, Bastiani M, Luetterforst R, Kirkham M, Kirkham A, Nixon SJ, Walser P, Abankwa D, Oorschot VM, Martin S, Hancock JF, Parton RG. PTRF-Cavin, a conserved cytoplasmic protein required for caveola formation and function. Cell 2008;132(1):113–124. [PubMed: 18191225]
6. Liu L, Pilch PF. A critical role of cavin (polymerase I and transcript release factor) in caveolae formation and organization. J Biol Chem 2008;283(7):4314–4322. [PubMed: 18056712]
7. Schnitzer JE, Oh P, Pinney E, Allard J. Filipin-sensitive caveolae-mediated transport in endothelium: reduced transcytosis, scavenger endocytosis, and capillary permeability of select macromolecules. J Cell Biol 1994;127:1217–1232. [PubMed: 7525606]
8. Singh RD, Puri V, Valiyaveettil JT, Marks DL, Bittman R, Pagano RE. Selective caveolin-1-dependent endocytosis of glycosphingolipids. Mol Biol Cell 2003;14(8):3254–3265. [PubMed: 12925761]
9. Sharma DK, Brown JC, Choudhury A, Peterson TE, Holicky E, Marks DL, Simari R, Parton RG, Pagano RE. Selective stimulation of caveolar endocytosis by glycosphingolipids and cholesterol. Mol Biol Cell 2004;15(7):3114–3122. [PubMed: 15107466]
10. Pelkmans L, Kartenbeck J, Helenius A. Caveolar endocytosis of simian virus 40 reveals a new two-step vesicular-transport pathway to the ER. Nature Cell Biol 2001;3:473–483. [PubMed: 11331875]
11. Orlandi PA, Fishman PH. Filipin-dependent inhibition of cholera toxin: evidence for toxin internalization and activation through caveolae-like domains. J Cell Biol 1998;141(4):905–915. [PubMed: 9585410]
12. Torgersen ML, Skretting G, van Deurs B, Sandvig K. Internalization of cholera toxin by different endocytic mechanisms. J Cell Sci 2001;114:3737–3742. [PubMed: 11707525]
13. Puri V, Watanabe R, Singh RD, Dominguez M, Brown JC, Wheatley CL, Marks DL, Pagano RE. Clathrin-dependent and -independent internalization of plasma membrane sphingolipids initiates two Golgi targeting pathways. J Cell Biol 2001;154:535–547. [PubMed: 11481344]

14. Cheng ZJ, Singh RD, Sharma DK, Holicky EL, Hanada K, Marks DL, Pagano RE. Distinct mechanisms of clathrin-independent endocytosis have unique sphingolipid requirements. Mol Biol Cell 2006;17:3197–3210. [PubMed: 16672382]
15. Kumari S, Mayor S. ARF1 is directly involved in dynamin-independent endocytosis. Nat Cell Biol 2008;10(1):30–41. [PubMed: 18084285]
16. Parton RG, Joggerst B, Simons K. Regulated internalization of caveolae. Journal of Cell Biology 1994;127(5):1199–1215. [PubMed: 7962085]
17. Tagawa A, Mezzacasa A, Hayer A, Longatti A, Pelkmans L, Helenius A. Assembly and trafficking of caveolar domains in the cell: caveolae as stable, cargo-triggered, vesicular transporters. J Cell Biol 2005;170(5):769–779. [PubMed: 16129785]
18. Minshall RD, Sessa WC, Stan RV, Anderson RG, Malik AB. Caveolin regulation of endothelial function. Am J Physiol Lung Cell Mol Physiol 2003;285(6):L1179–L1183. [PubMed: 14604847]
19. Pelkmans L, Fava E, Grabner H, Hannus M, Habermann B, Krausz E, Zerial M. Genome-wide analysis of human kinases in clathrin-and caveolae/raft-mediated endocytosis. Nature 2005;436(7047):78–86. [PubMed: 15889048]
20. Kirkham M, Fujita A, Chadda R, Nixon SJ, Kurzchalia TV, Sharma DK, Pagano RE, Hancock JF, Mayor S, Parton RG. Ultrastructural identification of uncoated caveolin-independent early endocytic vehicles. J Cell Biol 2005;168(3):465–476. [PubMed: 15668297]
21. Singh RD, Holicky EL, Cheng Z, Kim SY, Wheatley CL, Marks DL, Bittman R, Pagano RE. Inhibition of caveolar uptake, SV40 infection, and β1-integrin signaling by a non-natural glycosphingolipid stereoisomer. J Cell Biol 2007;176:895–901. [PubMed: 17371832]
22. Escriche M, Burgueno J, Ciruela F, Canela EI, Mallol J, Enrich C, Lluis C, Franco R. Ligand-induced caveolae-mediated internalization of A1 adenosine receptors: morphological evidence of endosomal sorting and receptor recycling. Exp Cell Res 2003;285(1):72–90. [PubMed: 12681288]
23. Upla P, Marjomaki V, Kankaanpaa P, Ivaska J, Hyypia T, vand der Goot FG, Heino J. Clustering induces a lateral redistribution of α2β1 integrin from membrane rafts to caveolae and subsequent PKC-dependent internalization. Mol Biol Cell 2004;15:625–636. [PubMed: 14657242]
24. Kolter T, Proia RL, Sandhoff K. Combinatorial ganglioside biosynthesis. J Biol Chem 2002;277(29): 25859–25862. [PubMed: 12011101]
25. Hakomori SI. Inaugural Article: The glycosynapse. Proc Natl Acad Sci U S A 2002;99(1):225–232. [PubMed: 11773621]
26. Wang X, Sun P, Al-Qamari A, Tai T, Kawashima I, Paller AS. Carbohydrate-carbohydrate binding of ganglioside to integrin alpha(5) modulates alpha(5)beta(1) function. J Biol Chem 2001;276(11): 8436–8444. [PubMed: 11118433]
27. Zheng M, Fang H, Tsuruoka T, Tsuji T, Sasaki T, Hakomori S. Regulatory role of GM3 ganglioside in alpha 5 beta 1 integrin receptor for fibronectin-mediated adhesion of FUA169 cells. J Biol Chem 1993;268(3):2217–2222. [PubMed: 8420989]
28. Todeschini AR, Hakomori S. Functional role of glycosphingolipids and gangliosides in control of cell adhesion, motility, and growth, through glycosynaptic microdomains. Biochim Biophys Acta 2008;1780:421–433. [PubMed: 17991443]
29. Iwamori M, Ohta Y, Uchida Y, Tsukada Y. Arthrobacter ureafaciens sialidase isoenzymes, L, M1 and M2, cleave fucosyl GM1. Glycoconjugate journal 1997;14(1):67–73. [PubMed: 9076515]
30. Singh RD, Liu Y, Wheatley CL, Holicky EL, Makino A, Marks DL, Kobayashi T, Subramaniam G, Bittman R, Pagano RE. Caveolar endocytosis and microdomain association of a glycosphingolipid analog is dependent on its sphingosine stereochemistry. J Biol Chem 2006;281:30660–30668. [PubMed: 16893900]
31. Stanley P, Ioffe E. Glycosyltransferase mutants: key to new insights in glycobiology. Faseb J 1995;9 (14):1436–1444. [PubMed: 7589985]
32. Parton RG, Molero JC, Floetenmeyer M, Green KM, James DE. Characterization of a distinct plasma membrane macrodomain in differentiated adipocytes. J Biol Chem 2002;277(48):46769–46778. [PubMed: 12356772]
33. Pol A, Martin S, Fernandez MA, Ingelmo-Torres M, Ferguson C, Enrich C, Parton RG. Cholesterol and fatty acids regulate dynamic caveolin trafficking through the Golgi complex and between the cell surface and lipid bodies. Mol Biol Cell 2005;16(4):2091–2105. [PubMed: 15689493]

34. Marks DL, Bittman R, Pagano RE. Use of Bodipy-labeled sphingolipid and cholesterol analogs to examine membrane microdomains in cells. Histochem Cell Biol 2008;130(5):819–832. [PubMed: 18820942]
35. Pagano RE, Martin OC, Kang HC, Haugland RP. A novel fluorescent ceramide analogue for studying membrane traffic in animal cells: accumulation at the Golgi apparatus results in altered spectral properties of the sphingolipid precursor. Journal of Cell Biology 1991;113(6):1267–1279. [PubMed: 2045412]
36. Takahashi M, Murate M, Fukuda M, Sato SB, Ohta A, Kobayashi T. Cholesterol controls lipid endocytosis through Rab11. Mol Biol Cell 2007;18(7):2667–2677. [PubMed: 17475773]
37. Ito M, Komori H. Homeostasis of cell-surface glycosphingolipid content in B16 melanoma cells. Evidence revealed by an endoglycoceramidase. J Biol Chem 1996;271(21):12655–12660. [PubMed: 8647878]
38. Ji L, Ito M, Zhang G, Yamagata T. The hydrolysis of cell surface glycosphingolipids by endoglycoceramidase reduces epidermal growth factor receptor phosphorylation in A431 cells. Glycobiology 1995;5(3):343–350. [PubMed: 7655171]
39. Tsai B, Gilbert JM, Stehle T, Lencer W, Benjamin TL, Rapoport TA. Gangliosides are receptors for murine polyoma virus and SV40. Embo J 2003;22(17):4346–4355. [PubMed: 12941687]
40. Hanada K. Sphingolipids in infectious diseases. Jpn J Infect Dis 2005;58(3):131–148. [PubMed: 15973004]
41. Simons K, Ehehalt R. Cholesterol, lipid rafts, and disease. J Clin Invest 2002;110(5):597–603. [PubMed: 12208858]
42. Duncan MJ, Shin JS, Abraham SN. Microbial entry through caveolae: variations on a theme. Cell Microbiol 2002;4(12):783–791. [PubMed: 12464009]
43. Lafont F, Abrami L, van der Goot FG. Bacterial subversion of lipid rafts. Curr Opin Microbiol 2004;7 (1):4–10. [PubMed: 15036133]
44. Richterova Z, Liebl D, Horak M, Palkova Z, Stokrova J, Hozak P, Korb J, Forstova J. Caveolae are involved in the trafficking of mouse polyomavirus virions and artificial VP1 pseudocapsids toward cell nuclei. J Virol 2001;75(22):10880–10891. [PubMed: 11602728]
45. del Pozo MA, Balasubramanian N, Alderson NB, Kiosses WB, Grande-Garcia A, Anderson RG, Schwartz MA. Phospho-caveolin-1 mediates integrin-regulated membrane domain internalization. Nat Cell Biol 2005;7(9):901–908. [PubMed: 16113676]
46. Miyagi T, Wada T, Yamaguchi K, Hata K, Shiozaki K. Plasma membrane-associated sialidase as a crucial regulator of transmembrane signalling. J Biochem 2008;144(3):279–285. [PubMed: 18632803]
47. Hakomori S. Tumor-associated carbohydrate antigens defining tumor malignancy: basis for development of anti-cancer vaccines. Adv Exp Med Biol 2001;491:369–402. [PubMed: 14533809]
48. Hettmer S, Ladisch S, Kaucic K. Low complex ganglioside expression characterizes human neuroblastoma cell lines. Cancer Lett 2005;225(1):141–149. [PubMed: 15922866]
49. Birkle S, Zeng G, Gao L, Yu RK, Aubry J. Role of tumor-associated gangliosides in cancer progression. Biochimie 2003;85(3–4):455–463. [PubMed: 12770784]
50. Guerrera M, Ladisch S. N-butyldeoxynojirimycin inhibits murine melanoma cell ganglioside metabolism and delays tumor onset. Cancer Lett 2003;201(1):31–40. [PubMed: 14580684]
51. Ling K, Doughman RL, Firestone AJ, Bunce MW, Anderson RA. Type I gamma phosphatidylinositol phosphate kinase targets and regulates focal adhesions. Nature 2002;420(6911):89–93. [PubMed: 12422220]
52. Puri V, Jefferson JR, Singh RD, Wheatley CL, Marks DL, Pagano RE. Sphingolipid storage induces accumulation of intracellular cholesterol by stimulating SREBP-1 cleavage. J Biol Chem 2003;278 (23):20961–20970. [PubMed: 12657626]
53. Ledeen RW, Yu RK. Gangliosides: structure, isolation, and analysis. Methods Enzymol 1982;83:139–191. [PubMed: 7047999]

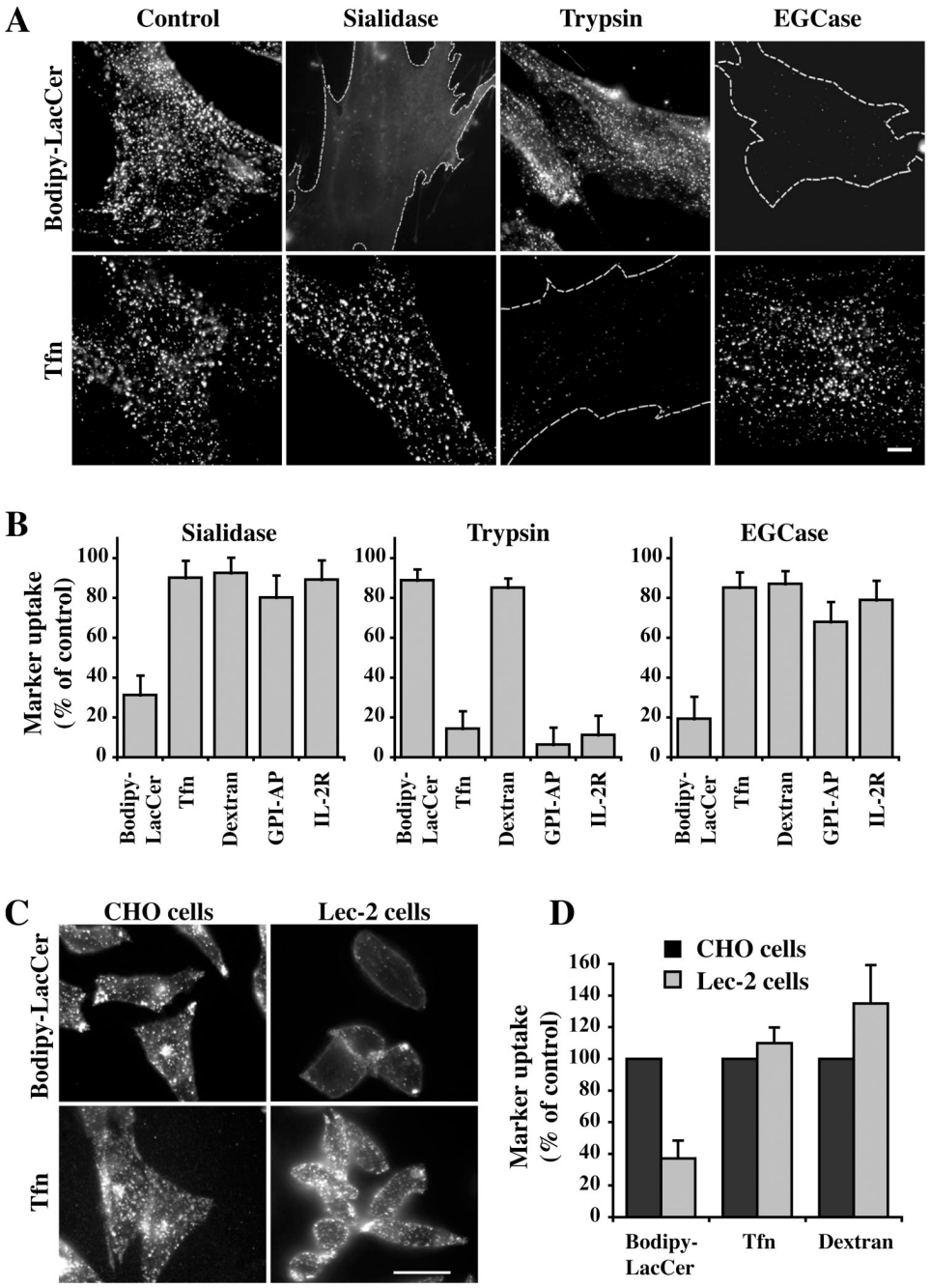

Fig 1. Effect of sialic acid depletion on endocytosis

(A,B) HSFs were preincubated for 30 min at 37°C without (Control) or with sialidase, trypsin, or EGCase, washed, and the internalization of Bodipy-LacCer, Tfn, Dextran, GFP-GPI, and IL-2β receptor were assessed after 5 min of endocytosis at 37°C. (A) Fluorescence micrographs showing the effects of sialidase, trypsin, or EGCase pretreatments on Bodipy-LacCer and Tfn uptake. Dotted lines outline the cells in field. (B) Uptake of multiple markers after 5 min of endocytosis at 37°C. Note the selective inhibition of endocytosis of Bodipy-LacCer (but not other markers) following pretreatment with sialidase or EGCase. Endocytosis was quantified by image analysis ($n \geq 30$ cells/marker in 3 independent experiments) and expressed as means ± SE relative to untreated control samples. See Fig. S2A for optimization of sialidase and

EGCase pretreatment times on Bodipy-LacCer endocytosis. (C,D) Endocytosis of Bodipy-LacCer, Tfn, and dextran in a mutant CHO cell line that has decreased levels of cell surface sialic acid. (C) Fluorescence micrographs of Bodipy-LacCer and Tfn in the CHO parental (Pro5) and Lec-2 mutant cells (defective in the transport of CMP-NeuAc into the lumen of the Golgi apparatus) after 5 min of endocytosis at 37°C. (D) Quantitation of uptake by image analysis ($n \geq 30$ cells/marker in 3 independent experiments). Bars, 10 μm.

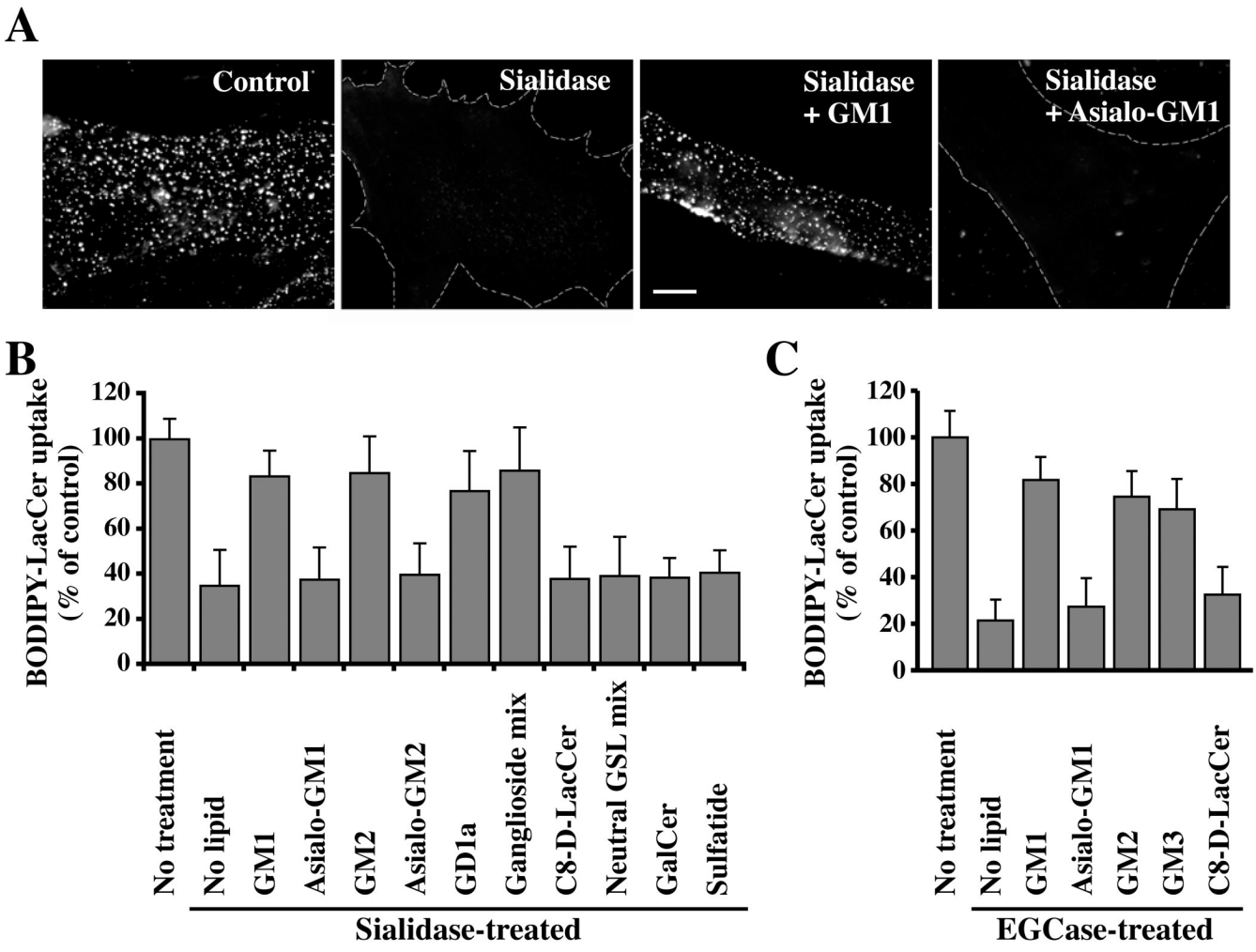

Fig. 2. Restoration of Bodipy-LacCer endocytosis in HSFs by sialic acid containing gangliosides

Cells were pretreated with sialidase (A,B) or EGCase (C) as in Fig. 1, washed, and pulse-labeled with Bodipy-LacCer to monitor uptake after 5 min of endocytosis at 37°C. In some instances the enzyme-pretreated cells were incubated for 30 min at 10°C with the indicated non-fluorescent lipid, washed, and subsequently pulse-labeled with Bodipy-LacCer as above. (A) Fluorescence micrographs showing inhibition of Bodipy-LacCer uptake by sialidase and restoration of endocytosis by GM_1 (but not asialo-GM_1) ganglioside. Bar, 10 μm. (B,C) Quantitative results for restoration of Bodipy-LacCer endocytosis by various lipids after sialidase or EGCase treatments. “No treatment,” refers to no enzymatic pretreatment; “No lipid” shows effect of enzymatic treatment without lipid addition. Values were quantified as in Fig. 1 ($n \geq 30$ cells/marker in 3 independent experiments) and are expressed as means ± SE relative to untreated control samples.

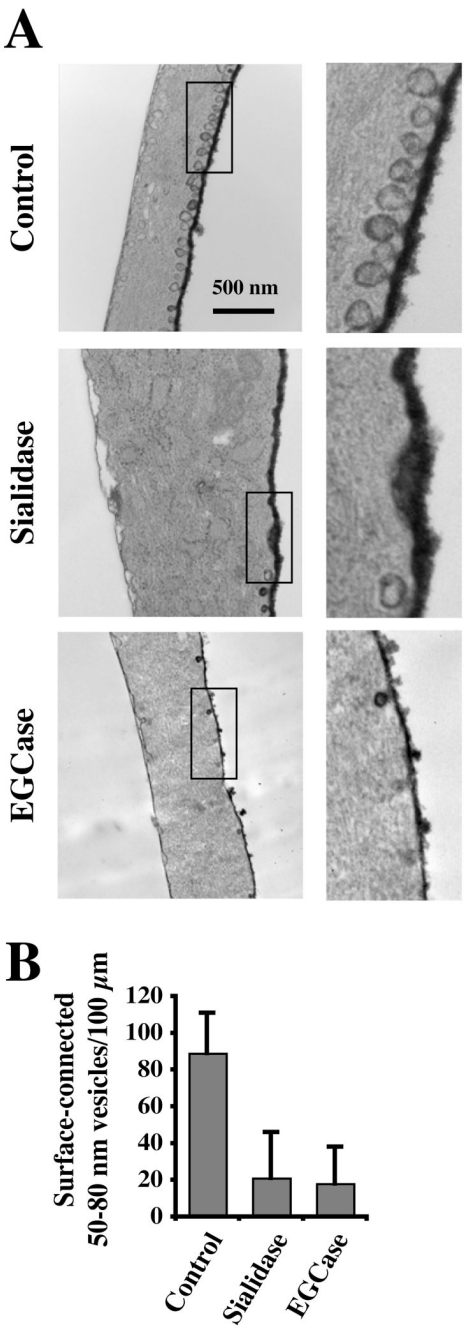

Fig. 3. Effect of sialidase and EGCase treatments on caveolae

(A) HSFs were untreated (Control) or treated for 30 min at 37°C with sialidase or EGCase, fixed, stained with ruthenium red to identify PM invaginations, and processed for transmission electron microscopy. Bar, 500 nm. (B) For quantitation, 50–80-nm diameter smooth, surface-connected vesicles within 0.5 μm of the cell surface were counted along the entire cell perimeter and are expressed (means ± SE) as number per 100 μm of length.

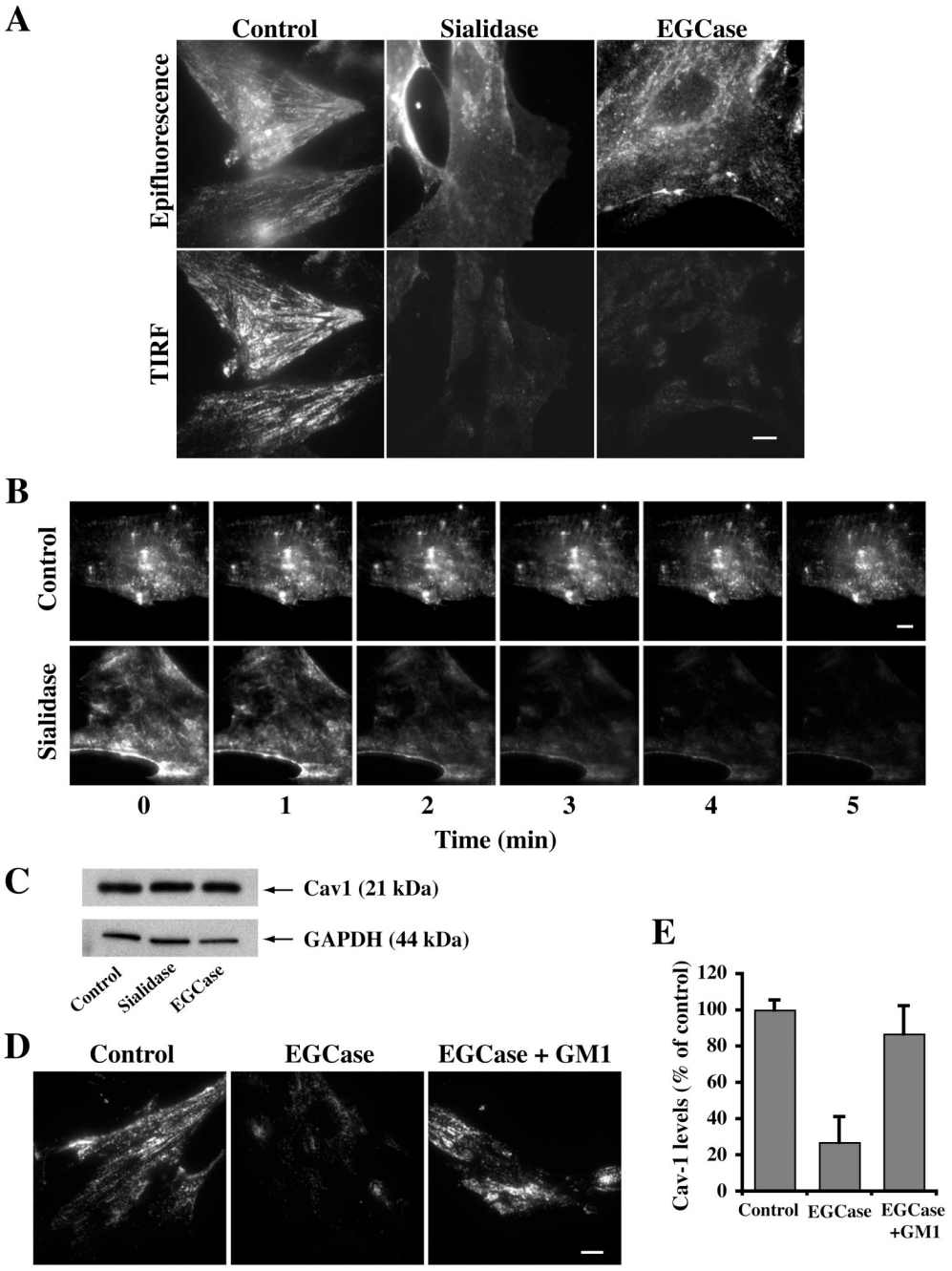

Fig. 4. Cav1 is lost from the PM following sialidase or EGCase treatments but is restored by incubation with exogenous GM_1 ganglioside at low temperature

(A) HSFs were untreated or treated with the indicated enzyme for 30 min at 37°C, fixed, immunostained for Cav1, and observed by epifluorescence or TIRF microscopy. Note the loss of Cav1 from the cell surface (TIRF images) in the treated cells. (B) Real time imaging of Cav1-GFP demonstrates redistribution of Cav1 from the cell surface to intracellular membranes during incubation with sialidase at 37°C. Indicated time points are taken from QuickTime movies. Control experiments using buffer alone showed no redistribution of Cav1-GFP over the same time period. (C) Total Cav1 levels by western blotting were not altered by sialidase or EGCase treatments. (D,E) Endogenous Cav1 redistributes back to the PM of

EGCase-treated cells following a 30 min incubation with exogenous GM_1 ganglioside at 10° C. Quantitation of TIRF signal for Cav1 in panel (E) was by image analysis ($n \geq 30$ cells/condition) and is expressed (mean ± SE) as a percent of controls. Bars, 10 μm.

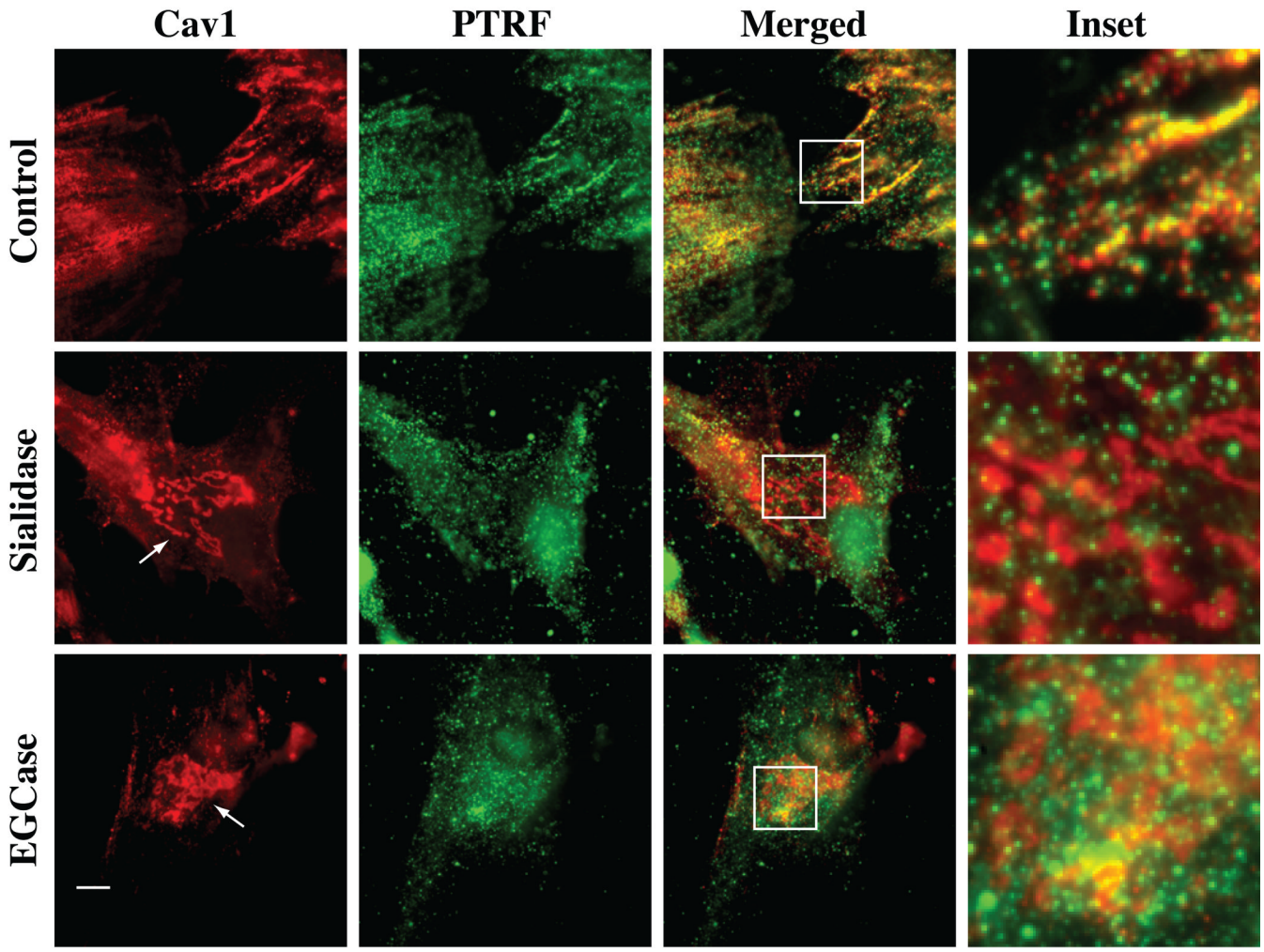

Fig. 5. Effect of sialidase or EGCase treatment on the distribution of Cav1 and PTRF-Cavin

HSFs were treated with or without the indicated enzyme for 30 min at 37°C followed by immunostaining of Cav1 (red) and PTRF-Cavin (green). Note the typical surface-like staining of Cav1 and extensive co-localization with PTRF-Cavin in control cells, while in sialidase- or EGCase-treated cells these proteins were non-overlapping and in different structures. Arrows indicate Golgi region. Bars, 10 μm.

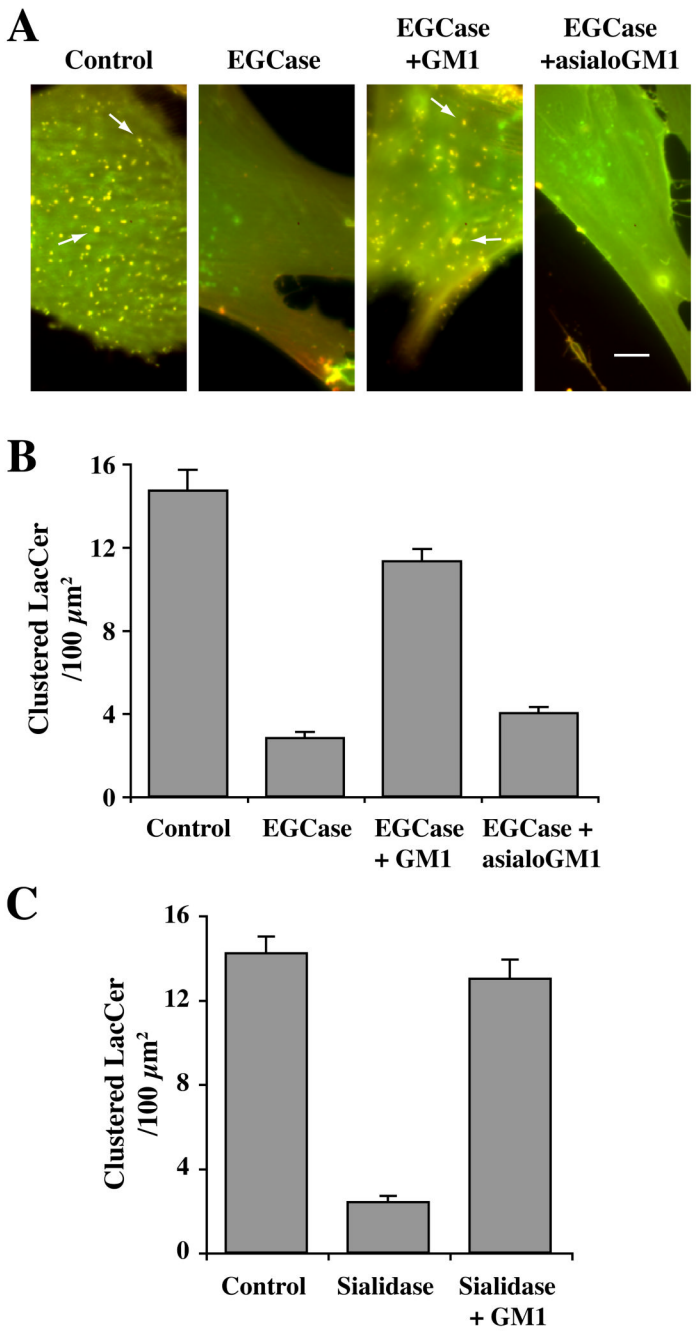

Fig. 6. Enzymatic cleavage of cell surface sialic acid residues abolished PM domains enriched in Bodipy-LacCer

HSFs were untreated (Control), or pretreated with EGCase (A,B) or sialidase (C) for 30 min at 37°C, followed by incubation with 2.5 μM Bodipy-LacCer for 30 min at 10°C. Cells were then washed and fluorescence images were acquired simultaneously at green and red wavelengths and merged. Imaging was carried out at low temperature to inhibit endocytosis. (A) Note the presence of yellow/orange micron size clusters in control cells (e.g., at arrows) whereas no such domains were observed in EGCase-treated cells (middle panels). PM domain formation was restored when the enzyme-treated cells were incubated for 30 min at 10°C with exogenous GM_1 ganglioside prior to incubation with Bodipy-LacCer (right panels). No

restoration of PM domains was seen using asialo-GM_1 in place of GM_1. Bars, 10 μm. See Fig. S3 for an image of BODIPY-LacCer-labeled sialidase-treated cells. In (B,C) the number of "patches" ≥ 1×1 μm were quantified by image analysis and are expressed per 100 μm^2 area (n ≥ 6 cells per condition in 2 or more independent experiments).

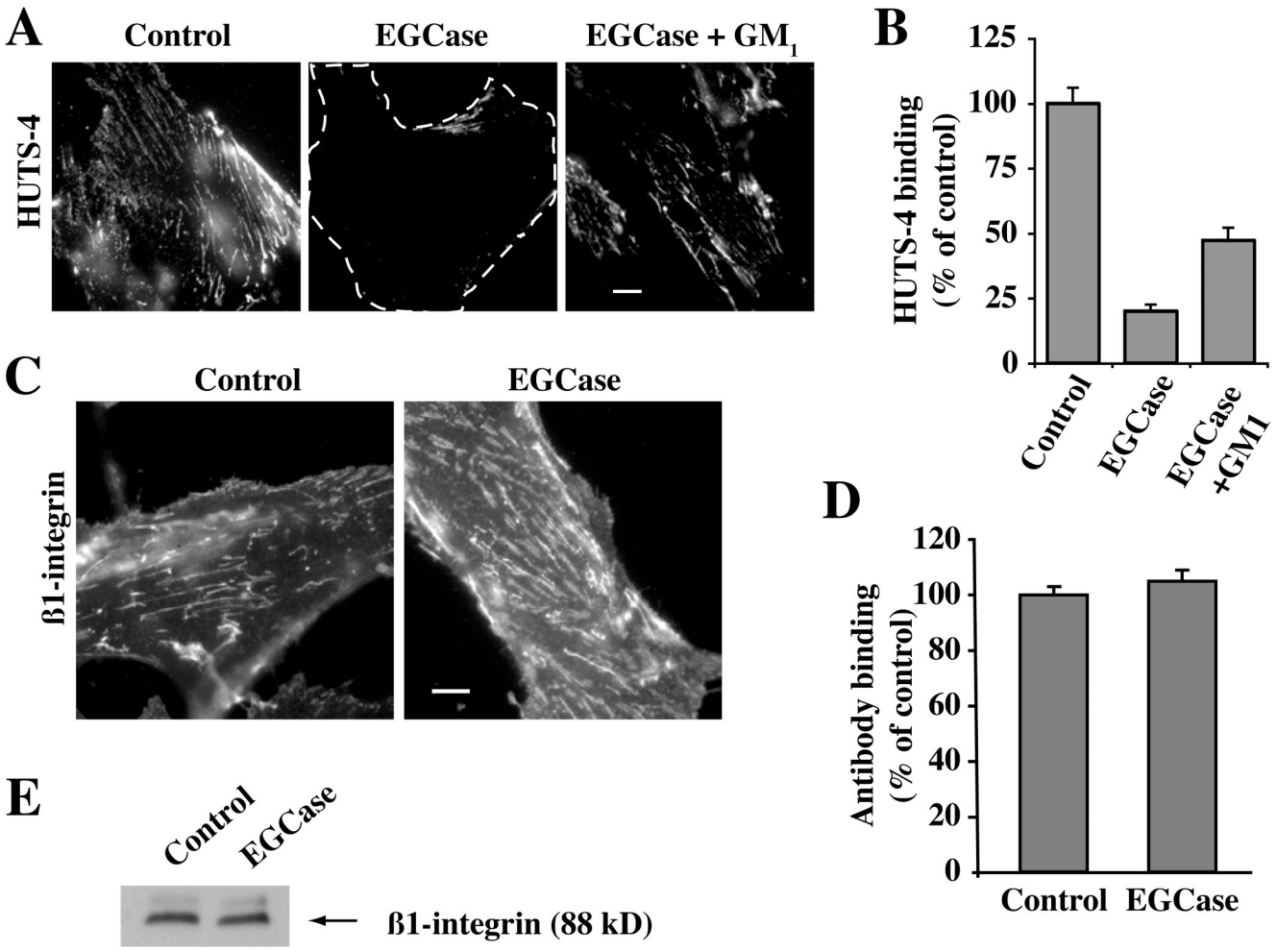

Fig. 7. Effect of EGCase treatment on β1-integrin levels and activation

HSFs were grown in serum-containing medium, washed, and were either untreated (Control) or pretreated with EGCase for 30 min at 37°C. (A,B) Control or EGCase treated cells were washed, warmed for 30 sec at 37°C, fixed, and immunostained with HUTS-4 mAb to detect activated β1-integrin. In one experiment the EGCase treated cells were subsequently washed and incubated for 30 min at 10°C with GM_1 ganglioside prior to HUTS-4 fixation and staining. In (B), images from the experiment in panel (A) were quantified as in panel by image analysis ($n \geq 50$ cells) and are expressed as a percent of untreated control samples (mean ± SE). (C,D) Live cells were stained for 30 min at 10°C using a β1-integrin FITC-labeled antibody (monitors both activated and non-activated β1-integrin), washed, and observed under the fluorescence microscope. No significant difference in fluorescence intensity between Control and EGCase treated cells ($n \geq 50$ cells/condition) was observed. (E) Cells treated as in (C,D) were lysed and blotted for β1-integrin (10 μg protein per lane). Bars, 10 μm.

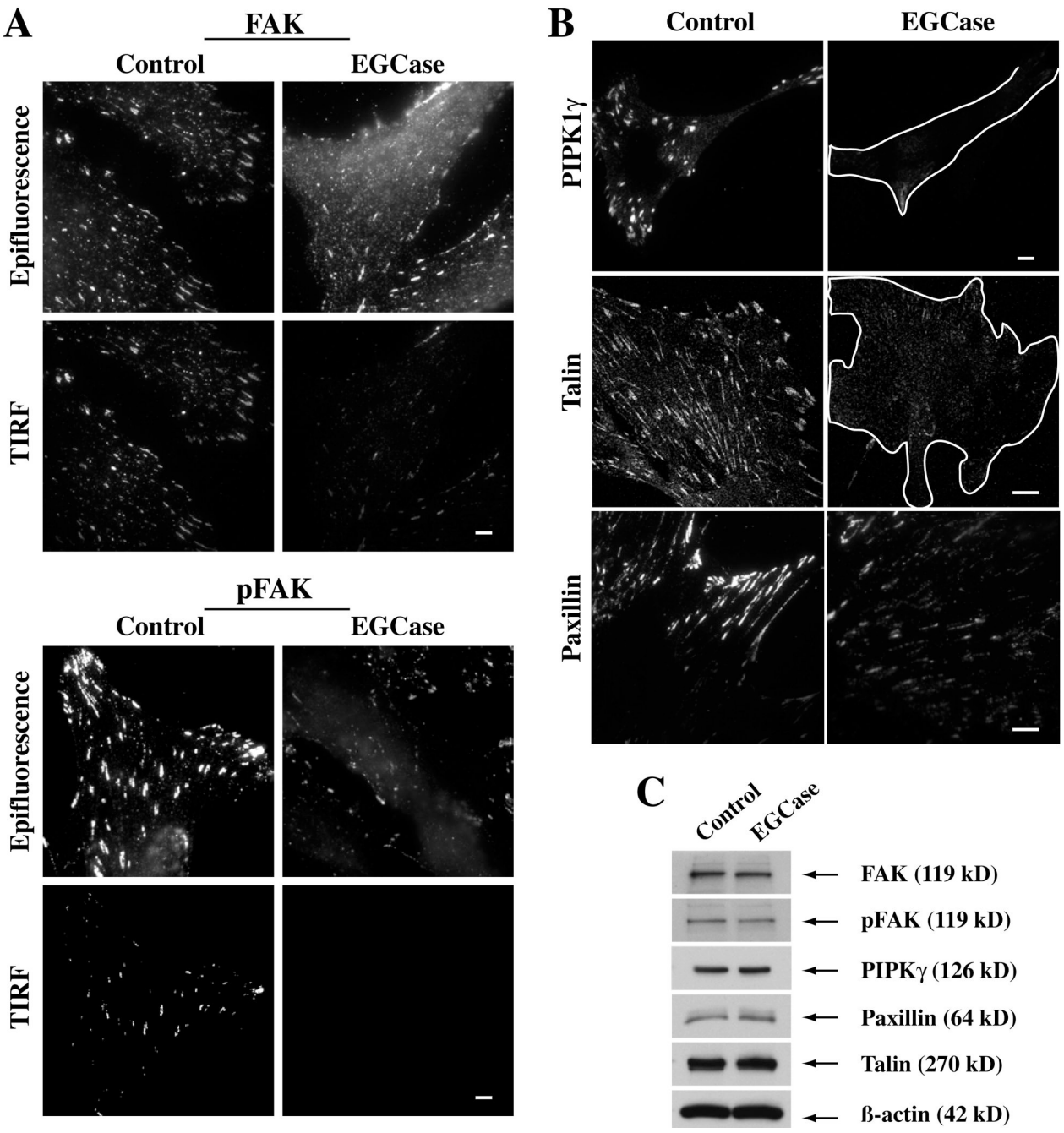

Fig 8. Effect of EGCase treatment of HSFs on focal adhesion components

(A) Cells were grown in serum-containing medium, washed, and subsequently were untreated (Control) or pretreated with EGCase for 30 min at 37°C. The basal level of FAK and pFAK (Y397) was then assessed by antibody staining using both epifluorescence and TIRF microscopy. (B) Parallel cell samples, grown under the same conditions, were immunostained for talin or paxilin. In the case of PIPK1γ cells were transfected overnight with HA-tagged PIPKIγ prior to EGCase treatment, fixation and immunostaining. PIPKIγ and talin images were by confocal microscopy; paxilin images were by TIRF microscopy. (C) In parallel dishes, cells were untreated (Control) or pretreated with EGCase for 30 min at 37°C, lysed, and cell lysates (10 µg protein per lane) were immunoblotted for various proteins as indicated. Bars, 10 µm.

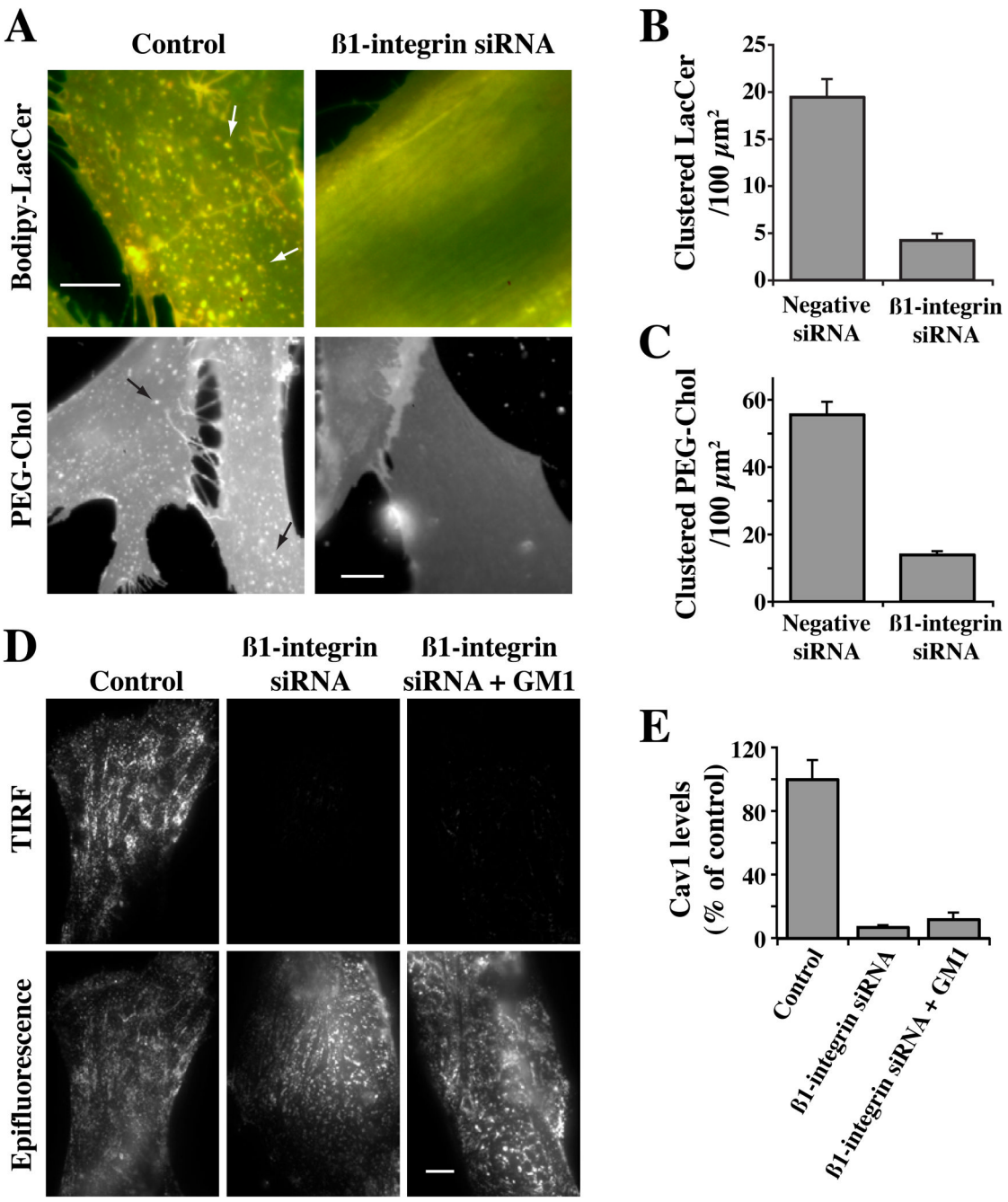

Fig. 9. Effect of β1-integrin knockdown on PM domains and the distribution of Caveolin-1

HSFs were transfected for 72 hrs with negative (Control) or β1-integrin siRNA (Supp. Fig. S4). (A–C) Cells were then incubated with Bodipy-LacCer or AF647-PEG-Chol to visualize PM clusters (e.g., at arrows of Control samples). In (B,C) the number of micron size clusters of Bodipy-LacCer or PEG-Chol were quantified as in Fig. 6. (D,E) Cells as above were fixed and immunostained for Cav1. Samples were then visualized by TIRF or epifluorescence microscopy. In (E) TIRF images from the experiment in panel (D) were quantified by image analysis ($n \geq 50$ cells) and are expressed as a percent of untreated control samples (mean ± SE). Bars, 10 μm